



**HAL**  
open science

## Assessment of sustainability on structure-optical properties of prismatic face ADP crystal at dynamic shocked conditions

A. Sivakumar, S.S. Jude Dhas, R. Suresh Kumar, A.I. Almansour, N. Arumugam, Shubhadip Chakraborty, S.A. Martin Britto Dhas

### ► To cite this version:

A. Sivakumar, S.S. Jude Dhas, R. Suresh Kumar, A.I. Almansour, N. Arumugam, et al.. Assessment of sustainability on structure-optical properties of prismatic face ADP crystal at dynamic shocked conditions. *Physica B: Condensed Matter*, 2022, 634, pp.413793. 10.1016/j.physb.2022.413793 . hal-03632738

**HAL Id: hal-03632738**

<https://hal.science/hal-03632738v1>

Submitted on 11 Apr 2022

**HAL** is a multi-disciplinary open access archive for the deposit and dissemination of scientific research documents, whether they are published or not. The documents may come from teaching and research institutions in France or abroad, or from public or private research centers.

L'archive ouverte pluridisciplinaire **HAL**, est destinée au dépôt et à la diffusion de documents scientifiques de niveau recherche, publiés ou non, émanant des établissements d'enseignement et de recherche français ou étrangers, des laboratoires publics ou privés.



Distributed under a Creative Commons Attribution - NonCommercial 4.0 International License

**CRedit Authorship contribution statement**

**A.Sivakumar:** Data analysis, Writing-original draft; **S.Sahaya Jude Dhas:** Visualization, Roles/Writing - original draft; , **Raju Suresh Kumar:** Formal Analysis, **Abdulrahman I. Almansour:** Formal Analysis; **Natarajan Arumugam:** Resources, **Shubhadip Chakraborty:** Formal analysis; **S.A.Martin Britto Dhas:** Investigation, Writing-review & editing.

Journal Pre-proof



22 transmittance with respect to the number of shock pulses. Optical microscopic images also  
23 authenticate the formation of defective surface morphology at shocked conditions. Furthermore,  
24 we have made the comparison of the optical transmission of the prismatic face with the  
25 previously published pyramidal face ADP crystal with respect to the number of shock pulses.

26 **Key-words:** Shock waves, ADP crystal, Prismatic face, Optical transmission, Defects, Structural  
27 properties

## 28 **1. Introduction**

29 In the process of trying to get to the bottom of what is the basis of the observed changes  
30 caused by the impact of shock waves on materials, it has been identified that there are a lot of  
31 fundamental modifications which enforce drastic characteristic transformations. Much of these  
32 experimental works have come about because, in recent times, there have been witnessed a few  
33 groundbreaking results that emerge out from research groups owing to their incredible  
34 commitment. Space environmental factors can possibly affect the characteristic nature of space  
35 materials when they encounter the space condition such as gamma rays, low temperature, shock  
36 waves and cosmic rays, etc [1-4]. Optical devices are used in space mission for electronic types  
37 of equipment and laser operating systems to determine the efficiency of lifetime of satellites and  
38 data communication [5,6]. If the above-mentioned environmental factors could really affect the  
39 materials, the optical instruments are prone to undergo critical condition such that the resultant  
40 performances of the device tend to decrease resulting in deterioration of their characteristic  
41 features. Non- linear optical (NLO) crystals are used as frequency converters and for many other  
42 electronic devices such as LIDAR, SONAR, in space, military and defense technological  
43 applications [7,8]. High optical transmission is one of the basic requirements for the applications

44 of converters because it plays a crucial role in laser frequency converter devices. Hence, the  
45 stability of optical transmission has a paramount role in space, military and defense applications.  
46 To overcome the above-mentioned drawbacks and find novel suitable space materials for space  
47 applications, shock wave recovery experiment is proven to be one of the key techniques [9,10].  
48 Because during the shock wave propagation on test material, it can experience a similar situation  
49 as that of the space environment exposed on the surface of the test material that can be  
50 accomplished in the indoor laboratories itself. The aftermath of shock wave impact can generate  
51 a lot of usual and unusual effects on materials. Therefore, experimental investigations on  
52 crystalline and non-crystalline materials after the shock wave exposure have been witnessed to  
53 be consistently going up such that it is positioned to be a prominent research topic in current  
54 years [11-15]. At shock wave loaded conditions, micro and macro-level structural defects can be  
55 developed on material surfaces. In addition to that, grain boundaries diffusion, re-crystallization  
56 and phase transformation can also occur which are highly associated with the nature of material's  
57 response to high-pressure and temperature [16,17]. It is well authenticated that if crystallographic  
58 structural properties are altered, all kinds of dynamic physical properties such as thermal,  
59 electrical and optical properties are found to be greatly affected. Hence, research on finding the  
60 materials of crystallographic phase stability under harsh environmental conditions has attained  
61 the position of imploding a paradigm shift to be termed as one of the top-class research themes in  
62 recent years.

63 Over the years, a lot of NLO materials have been found for high-power laser applications  
64 whereas potassium dihydrogen phosphate (KDP) and ammonium dihydrogen phosphate (ADP)  
65 crystals are being regarded as the legendary research materials because of their exceptional

66 characteristic nature of growth and physical properties [18-20]. Among the two crystals, KDP's  
67 crystal structure [21] and other physical properties such as surface properties [21], optical  
68 transmission [21], dielectric constant [22], thermal diffusivity [23] and optical band gap energy  
69 [24] have been extensively studied by our research group at dynamic shock wave loaded  
70 conditions. In the case of ADP crystal, the crystal structure of the pyramidal face and other  
71 physical properties have been studied at shocked conditions [25-27]. Sivakumar et al have  
72 demonstrated the significant improvement in the degree of crystalline nature of the pyramidal  
73 face of ADP crystal at shocked conditions and ADP's surface properties, dielectric constant [25],  
74 optical transmission [26], thermal diffusivity [23] are found to have enhanced. Joshi *et al* have  
75 conducted the shock wave recovery experiment on Glutamic acid doped ADP crystal and found  
76 the reduction of the degree of crystalline nature and dielectric constant at shocked conditions  
77 [27]. Furthermore, our research group has examined a few other technologically potential single  
78 crystals' optical properties such as benzyl [28], tri-glycine sulfate [29], potassium sulfate [30],  
79 copper sulfate pentahydrate [31] crown ether magnesiuchloride potassium thiocyanate [32] and  
80 found several interesting results. Based on the available literature reports, the prismatic face  
81 ADP single crystal's physical properties have not yet been reported at shocked conditions.  
82 Therefore, the prismatic ADP crystal is considered for the current investigation on the stability of  
83 structural and optical transport properties under the condition of various counts of shock waves  
84 exposed in such a way that the observed results could provide the possible key evidence on the  
85 applicability of the crystal for space applications.

86 On those lines, we have analyzed the stability of crystal structure and degree of  
87 crystalline nature of the prismatic ADP crystal at shocked conditions by X-ray diffraction and

88 Raman spectroscopic techniques. Furthermore, the optical transmittance profile has been  
89 analyzed by UV-Vis spectrometer and the stability profiles have been established with respect to  
90 the number of shock pulses.

## 91 **2. Crystal growth and Shock wave loading methodology**

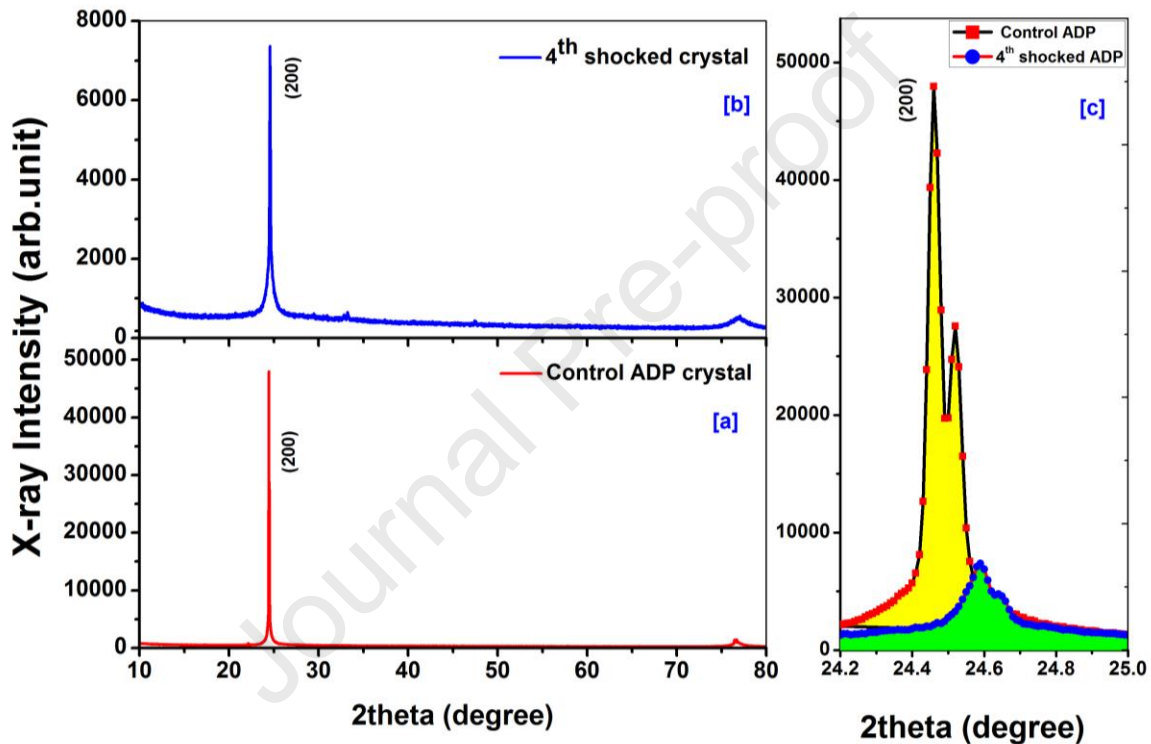
92 The crystal growth details of ADP crystal have been discussed in our previous  
93 publications [25,26]. For the present experiment, cut and polished prismatic ADP crystals of  
94 1mm thickness have been used. A pressure-driven tabletop Reddy tube, which was indigenously  
95 designed in our laboratory, has been made use of to generate the shock waves and the details of  
96 the shock tube has been published elsewhere [33]. In the present experiment, shock wave of  
97 Mach number 1.7 equivalent to the transient pressure of 1.0 MPa has been utilized for the  
98 assessment of the stability of crystal structure and optical properties of the prismatic ADP  
99 crystal. Five identical crystals have been loaded with shock pulses of 0,1,2,3 and 4, respectively.  
100 After shock wave loading, the respective crystals have been subjected to the studies of stability  
101 of crystal structure and optical transmission.

## 102 **3. Results and Discussion**

### 103 **3.1 X-ray diffraction analysis**

104 In the present experiment, Powder X-ray diffractometry (Rigaku – SmartLab X-ray  
105 Diffractometer, Japan) has been utilized to analyze the structural properties of the prismatic ADP  
106 crystal at shocked conditions. CuK $\alpha$  as the X-ray source ( $\lambda = 1.5407 \text{ \AA}$ ) of radiation and 1D  
107 detector have been utilized. Before loading the shock waves on the test sample, the control test  
108 sample's XRD pattern has been recorded and the obtained XRD pattern is presented in Fig.1a.

109 As seen in Fig.1a, the test sample has only one strong diffraction peak at  $24.461^\circ$  and the  
 110 corresponding diffraction position belongs to (200) crystallographic plane in the tetragonal  
 111 crystal structure and the diffraction angle position is well-matched with JCPDS – 85-0815. It is  
 112 noteworthy to mention that the crystal has only one diffraction plane with the specific orientation  
 113 (200) and no other considerable diffraction planes have been observed.



114

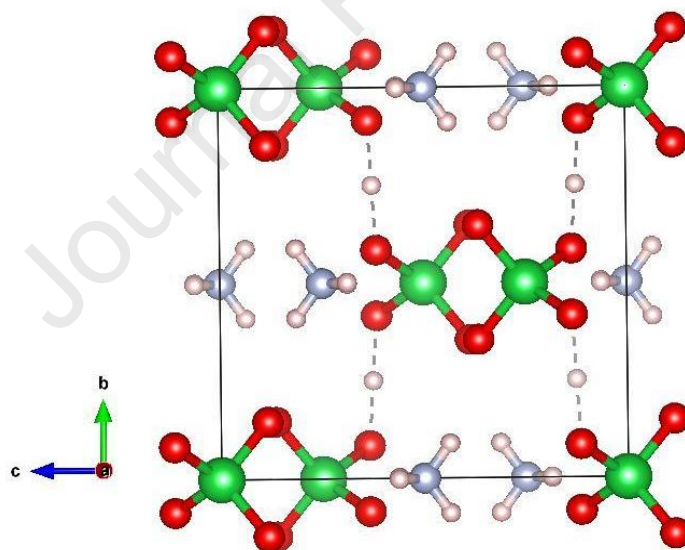
115 Fig.1 XRD pattern of the control and shocked prismatic face of ADP crystals

116 Furthermore, the observed control sample's diffraction peak (200) has very low full-  
 117 width half maximum and high peak intensity which clearly demonstrate that the test sample has  
 118 good crystalline nature. At shocked conditions ( especially at the 4<sup>th</sup> shock), considerable  
 119 changes are noticed in the intensity of diffraction peak and full-width half maximum that have  
 120 been significantly altered due to the influence of shocks which have to be considered to draw the



121 impact of shock waves on the structural properties of the prismatic ADP crystal. As the test  
122 sample is a single crystal, the intensity of the recorded XRD pattern must be taken into the  
123 account in order to get a clear picture on the impacted changes imposed on the crystal in terms of  
124 its structure and degree of crystallinity because of shock waves. As seen in Fig.1b, the shocked  
125 sample shows the retention of (200) crystalline plane and there is no new diffraction peak  
126 observed. Hence, at the first screening of the observed XRD pattern, it is obvious that the  
127 tetragonal crystal structure has not undergone any crystallographic phase transitions at shocked  
128 conditions. KDP family of crystals undergo crystallographic phase transitions at high-pressure  
129 and high-temperature conditions [34,35]. Takanori Fukami et al have demonstrated the  
130 crystallographic phase transition from the tetragonal  $I-42d$  to the monoclinic  $P2_1c$  at about 453 K  
131 [34]. Yan Ren et al have found the monoclinic KDP crystal at 1.9 GPa [35]. In addition to that, it  
132 is worthwhile to note that potassium sulfate crystal undergoes the changes from the  
133 orthorhombic to the hexagonal crystal phase transitions at the first shocked conditions and retain  
134 the orthorhombic structure at the 2<sup>nd</sup> shocked conditions [30]. But, in the present case, the  
135 substantial reduction of diffraction peak intensity is noticed which may be due to the formation  
136 of the lattice defects, changes in bonding schemes, misalignment of atomic lattice planes and  
137 deformations impacted by the shocks which have been also obtained quite similarly for the  
138 prismatic face of KDP crystal in such conditions [21]. Therefore, substantiation could be arrived  
139 at for the stability of the tetragonal crystal structure at post-shock conditions, but the degree of  
140 crystallinity is unstable at shocked conditions. Apart from the function of the crystal structure,  
141 the degree of crystalline nature also has the significant contribution in application point of view  
142 since most of the crystalline properties such as transmittance; thermal conductivity and dielectric  
143 constant are significantly altered with respect to the degree of crystalline nature [23]. Followed

144 by the X-ray diffraction intensity changes, the diffraction angle position also shows a  
 145 considerable change at shocked conditions. Initially, the most intense diffraction peak (200) is  
 146 located at  $24.461^\circ$  and at the 4<sup>th</sup> shocked condition; it experiences a quite higher angle diffraction  
 147 shift that is located at  $24.596^\circ$ . The observed diffraction angle shift of the (200) plane may be  
 148 due to the compression of hydrogen bonds such as N–H•••O and O–H•••O as well as crystal unit  
 149 volume by the impact of shock waves [19, 25]. In addition to that, the title crystal belongs to the  
 150 hydrogen bond family of crystals and the hydrogen bonds have high susceptible nature at high-  
 151 temperature and high-pressure conditions [36,37]. As per the crystal structure of the prismatic  
 152 face ADP crystal, N–H•••O is connected to  $(\text{NH}_4)^4$   $(\text{PO}_4)^3$  and O–H•••O lies between  $(\text{PO}_4)^3$   
 153 groups and the corresponding crystal packing along with (200) plane is presented in Fig.2.



154

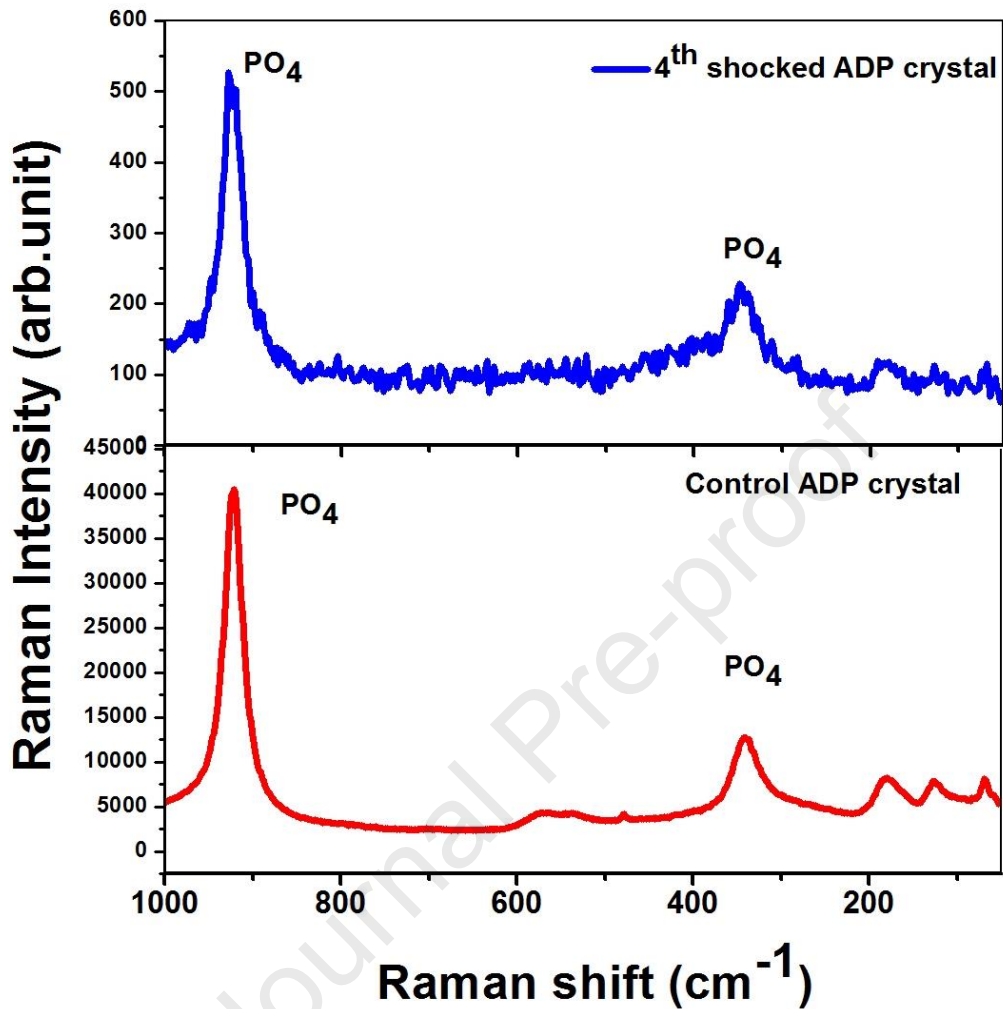
155 Fig.2 Crystal packing of ADP crystal along the (200) plane

156 As reflected in Fig.2, the prismatic face of ADP crystal comprises of alternative array of  
 157 anions and cations contributing to the growth habit of the crystal as against the pyramidal face

158 that has two hydrogen bonds which are highly susceptible at high-pressure and high-temperature  
159 as well as at dynamic shocked conditions. In addition to that, the total bond strength of the  
160 prismatic face ADP crystal (0.7282) is significantly low compared to the pyramidal face ADP  
161 crystal (1.6341) [38]. So that, it may not sustain the original crystalline state with specific atomic  
162 positions at shocked conditions and as a result it may produce the displacement of anions and  
163 cations including bond length changes from the original positions which may enable the loss of  
164 crystal symmetry and enhance the deformation levels in the test sample. Due to such changes,  
165 the net degree of crystalline nature of the prismatic plane in the crystal has faced a remarkable  
166 influence in the physical properties of the crystal.

### 167 **3.2 Raman Spectroscopic analysis**

168 Raman spectroscopic study has been performed to get deep in-sights on the structural  
169 properties of the test sample and the obtained Raman spectra of the control and shocked samples  
170 are presented in Fig.3. As it is known, ADP crystal is built by  $(\text{NH}_4)^+$  and  $(\text{PO}_4)^{3-}$  groups and it  
171 has two types of hydrogen bonds that are  $\text{N}-\text{H}\cdots\text{O}$  and  $\text{O}-\text{H}\cdots\text{O}$  which hold the major  
172 contribution to the structural properties of ADP crystal.



173

174

Fig.3 Raman spectra of the control and shocked prismatic face of ADP crystal

175

176

177

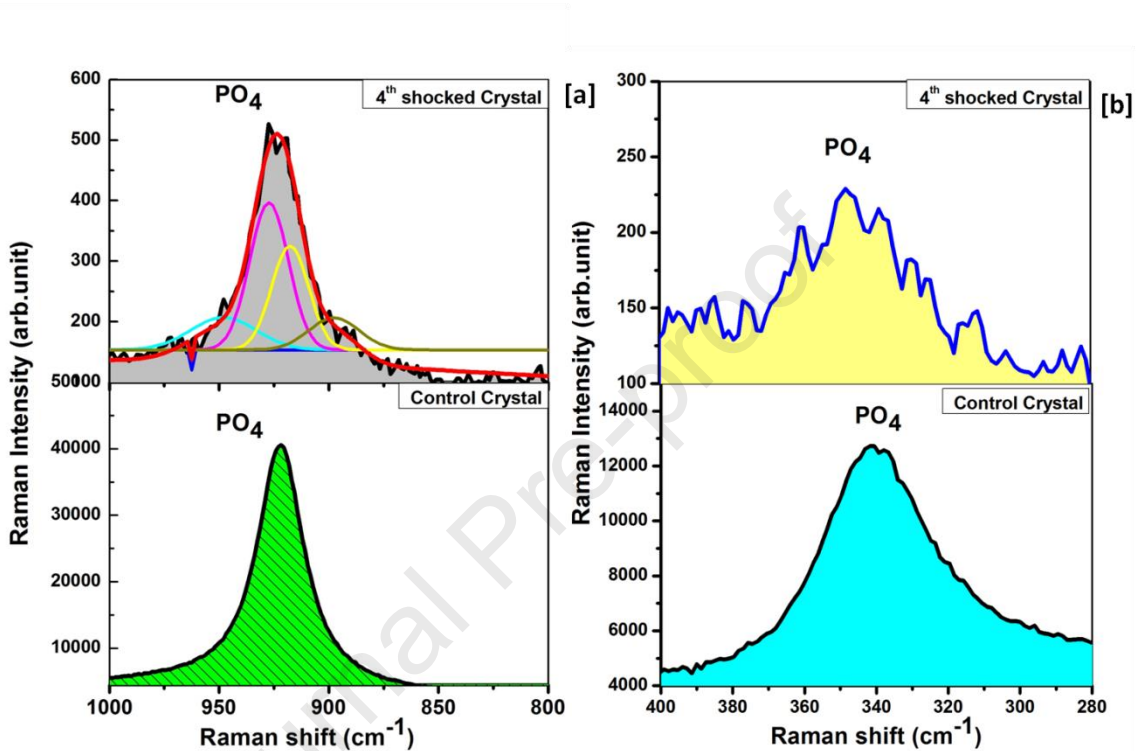
178

179

180

As seen in Fig.3, the control sample's Raman spectrum has the intense typical characteristic of  $\text{PO}_4$  tetrahedral Raman bands which are located at  $923 \text{ cm}^{-1}$  (bending mode) and  $339 \text{ cm}^{-1}$  (stretching mode) which are well-matched with the observations of the previous publications [39,40]. The observed characteristic  $\text{PO}_4$  Raman bands of the control sample clearly demonstrate that they belong to the tetragonal crystal structure. Furthermore, the appearance of the intense Raman bands shows that the test sample has good crystalline nature i.e. without any

181 surface defects. Under shock loadings, substantial changes are identified in terms of peak  
 182 intensity and peak splitting of PO<sub>4</sub> Raman bands and the zoomed-in version of the Raman bands  
 183 are presented in Fig.4 for a better visibility.

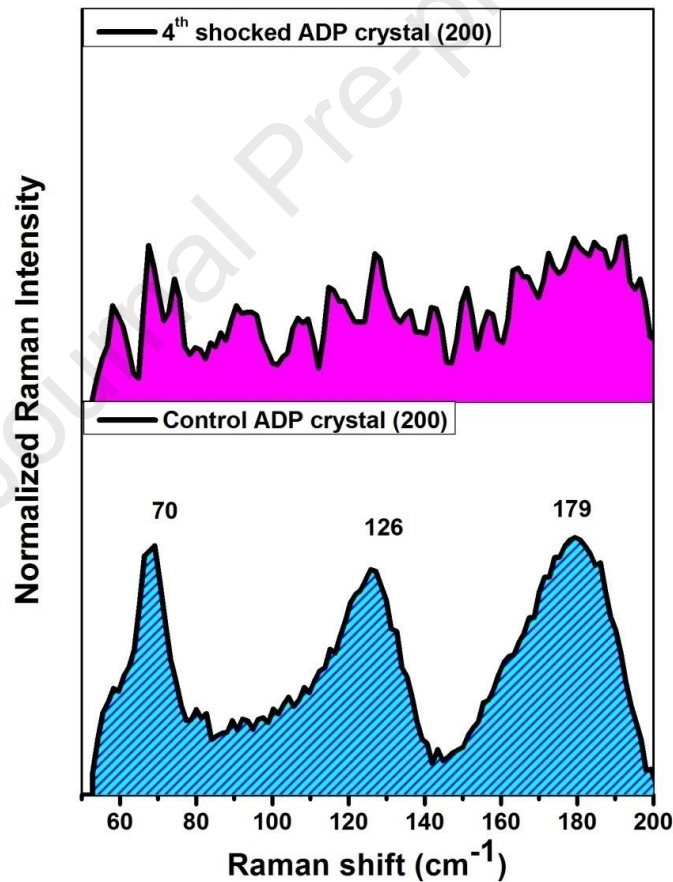


184

185 Fig.4 Zoomed-in versions of the PO<sub>4</sub> Raman bands for the control and shocked prismatic face of  
 186 ADP crystals

187 As seen in Fig.3a, ADP crystal's characteristic Raman band of asymmetric stretching PO<sub>4</sub>  
 188 has a single peak without peak splitting that could be noticed. But at shocked conditions, the  
 189 asymmetric stretching PO<sub>4</sub> Raman band exhibits a remarkable reduction of peak intensity and  
 190 peak splitting which clearly emphasize the formation of the distorted tetrahedral PO<sub>4</sub> and hence  
 191 the prismatic face of ADP crystal adopts a new structural configuration with different bond  
 192 lengths and bond angles along with different atomic sites which may induce the distortion of the

193 tetragonal crystal structure and the resultant is observed as a decrease in the degree of  
194 crystallinity for the after-shock specimen which is in good agreement with the results of XRD.  
195 In addition to that, the symmetric Raman band of  $\text{PO}_4$  at  $339\text{cm}^{-1}$  shows the similar results as that  
196 of the asymmetric  $\text{PO}_4$  at shocked conditions. Hence it is clear that, at shocked conditions,  
197 structural distortions have occurred in ADP crystal due to the instability of the tetragonal crystal  
198 structure [41]. In addition to that, the lattice Raman modes must be analyzed for a better  
199 elucidation of the actual crystal structure of ADP crystal and hence, the lattice Raman modes of  
200 the control and shocked crystals are presented in Fig.5.



201

202

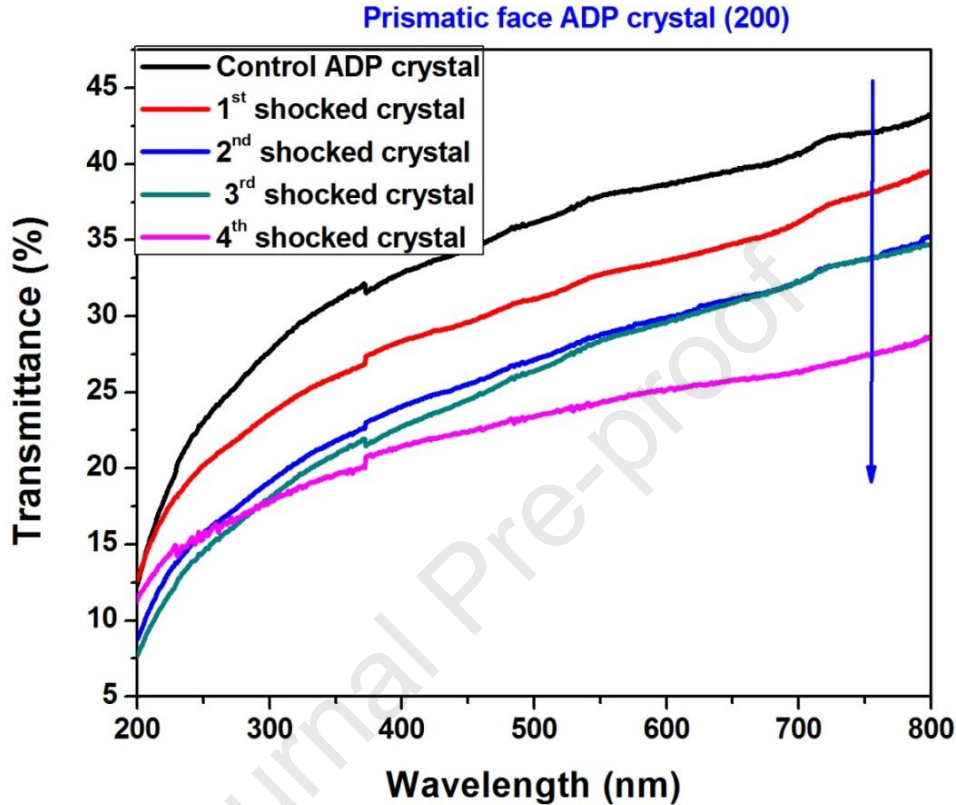
Fig.5 Lattice Raman modes of the control and the prismatic face of ADP crystal

203 As seen in Fig.5, the control crystal has well-defined three lattice Raman modes at 70  
204  $\text{cm}^{-1}$ ,  $126 \text{ cm}^{-1}$ , and  $179\text{cm}^{-1}$ , respectively and the lattice Raman band positions are well  
205 corroborated with the results of the previous publications [39,40] such that the Raman modes  
206 corresponding to the lattice vibrations of the crystal are due to the absorption or emission of  
207 optical phonons. At shocked conditions, the initial signatures such as lattice Raman mode pattern  
208 and intensities are destroyed which are the non-debatable proofs for the formation of the  
209 distorted tetragonal crystal structure at shocked conditions. On the other hand, there is neither  
210 crystallographic phase transition nor mixed phase formation has occurred at shocked conditions.

### 211 3.3 UV-Visible spectral studies

212 For non-linear optical materials, wide optical transmittance window and high optical  
213 transmittance are the major requirements for the industrial applications and hence the crystal  
214 growers have taken significant effort to grow crystals of high optical transmittance. But, while  
215 suggesting a particular functional material for industrial applications, the sustainability of the  
216 optical properties should also be measured at high-pressure and high-temperature environments  
217 for a better understanding of the scale of workability of the material. If the optical transmittance  
218 window and optical transmittance percentage are changed by the external parameters such as  
219 high-pressure and high-temperature or by sudden dynamic impact, the output of the electronic  
220 devices will vary significantly. In the case of the materials of second harmonic generation, the  
221 efficiency of the harmonic generation is significantly altered as and when the surface defects and  
222 structural defects are induced by shock waves so that we have measured the stability of the  
223 optical transmittance at shocked conditions and corresponding optical transmittance profiles are  
224 presented in Fig.6 wherein the observed pattern of optical transmittance is found to be well-

225 matched with the experimental data of the previous publications [26]. As seen in Fig.6, the  
 226 control sample has 36 % optical transmittance at 500 nm.



227

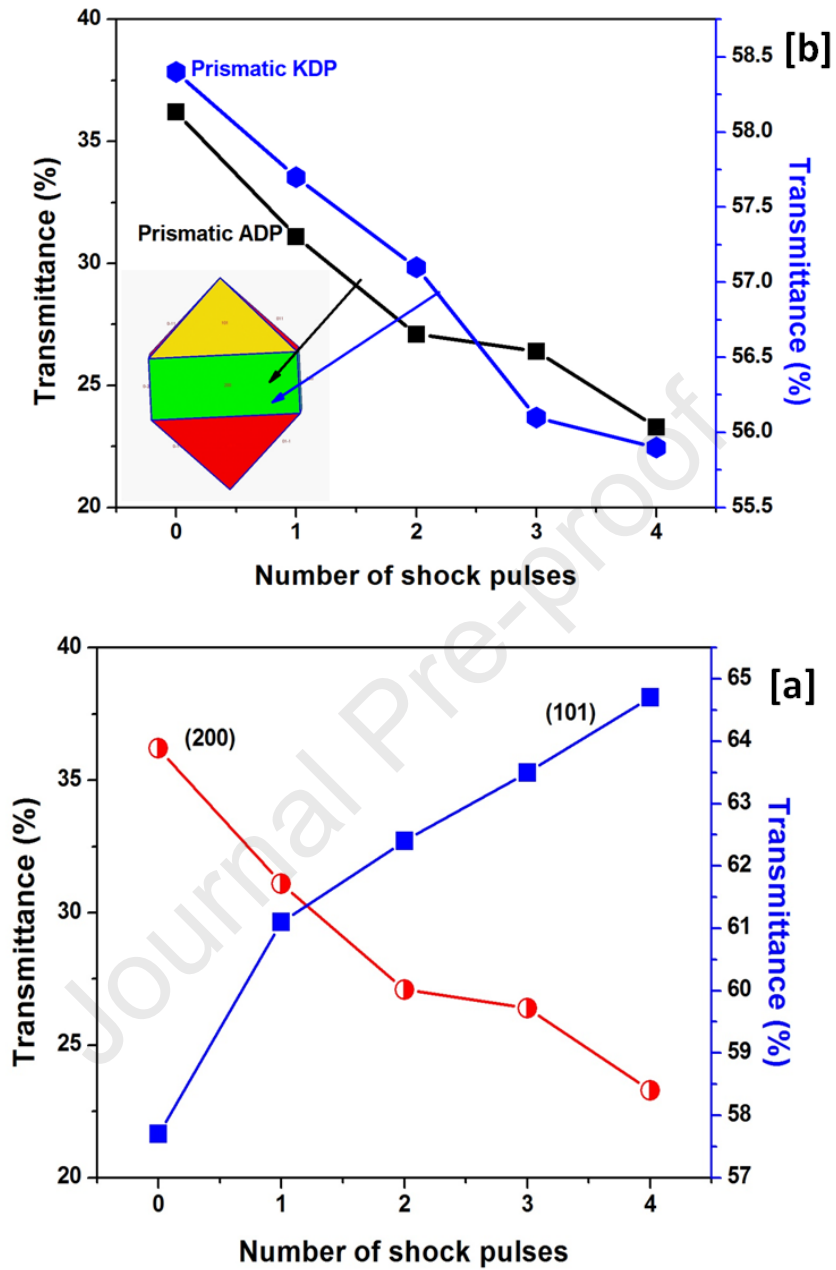
228 Fig.6. The profiles of optical transmittance of the control and shocked prismatic face of ADP  
 229 crystals

230 At shocked conditions, the optical transmittance has linearly reduced with respect to the  
 231 number of shock pulses and the corresponding plot is portrayed in Fig.7. The downward trending  
 232 of the optical transmittance of the test crystal may be due to the formation of lattice  
 233 deformations, distortion of crystal structures and surface defects. Similar results have been  
 234 observed for potassium dihydrogen phosphate [21], tri-glycine sulfate [29] at shocked  
 235 conditions. For a better understanding of the optical properties of ADP crystal in terms of its



236 sustainability with respect to the faces, we have made a systematic comparison of the percentage  
237 of optical transmittance for the prismatic and the pyramidal faces at shocked conditions and the  
238 corresponding plots are depicted in Fig.7a and 7b.

239 As seen in Fig.7a, optical transmittance of the (200) plane for the crystal has reduced  
240 with respect to the number of shock pulse whereas optical transmittance of the (101) plane has  
241 increased which has been previously reported [26]. The prismatic face of ADP and KDP [21]  
242 crystals' optical transmittance stability profiles are presented in Fig.7b. As seen in Fig.7b, both  
243 the crystals follow the downward trending percentage of optical transmittance with respect to the  
244 number of shock pulses. But KDP crystal shows very fine changes in the optical transmittance  
245 while compared to the prismatic face of ADP crystal. For example, the face of the KDP crystal  
246 shows the reduction of optical transmittance from 58% to 55.9% at the 4<sup>th</sup> shocked condition.  
247 Whereas the prismatic face of ADP crystal shows the reduction of optical transmittance from  
248 36% to 23.9% at the 4<sup>th</sup> shocked condition and hence, we consider that the prismatic face of KDP  
249 crystal has little higher shock resistance than that of the prismatic ADP crystal.



250

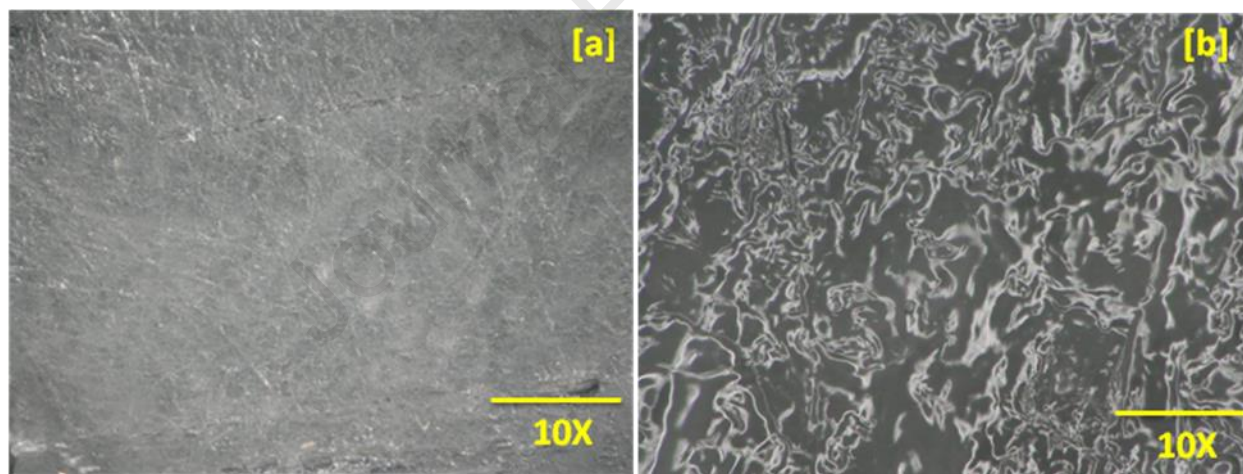
251 Fig.7. The profiles of optical transmittance of the control and shocked crystals (a) (200) and

252 (101) planes of ADP crystals (b) (200) plane of ADP and (200) plane for KDP crystal

253

### 254 3.4 Optical Microscopic Images

255 Furthermore, we have obtained the optical microscopic images to get the possible  
256 insights about the surface morphological changes of the prismatic ADP crystal at shocked  
257 conditions. As seen in Fig.8a, the control crystal's surface has a flat and smooth morphology.  
258 But at the 4<sup>th</sup> shocked condition, the test crystal's surface shows significant changes in the form  
259 of surface defects and the corresponding micrograph is presented in Fig.8b. The formation of  
260 surface defects may also have the equal contribution for the reduction of optical transmittance  
261 due to scattering that is followed by the loss of degree of crystalline nature and such surface  
262 defects formation and loss of optical transmittance have been witnessed for potassium  
263 dihydrogen phosphate and Tri-glycine sulfate crystals at shocked conditions [21,29].



264  
265 Fig.8 Optical micrographs of the prismatic ADP crystal (a) the control (b) the 4<sup>th</sup> shocked ADP

### 266 4. Conclusion

267 On summarizing the present research work, an organized assessment has been carried  
268 out on the nature of crystallinity and the stability of the optical transmittance of the prismatic

269 face ADP crystal at dynamic shocked conditions and the corresponding diffraction, spectroscopic  
270 results have been investigated. The observed X-ray diffraction and Raman spectroscopic results  
271 show the formation of the distorted tetragonal crystal structure at shocked conditions due to the  
272 noteworthy reduction of intensity of the diffraction peaks and complete modification of the  
273 lattice Raman modes. The analysis retrieved from UV-Visible spectrometer clearly discloses the  
274 optical linearly that decreases in terms of percentage in accordance with the number of shocks  
275 because of the formation of defects in the crystal structure and hence the prismatic face ADP  
276 crystal might not be a potential material for high-temperature and high-pressure environmental  
277 applications. In addition to that, optical microscopic images also provide the possible evidence  
278 for the formation of surface defects at shocked conditions. It could be noted that the prismatic  
279 face KDP crystal has high shock resistance than that of the prismatic face ADP crystal so that the  
280 prismatic face KDP crystal can be used for high-temperature applications.

### 281 **Conflicts of interest**

282 The authors declare that they have no conflict of interest.

### 283 **Acknowledgements**

284 The authors thank Department of Science and Technology (DST), India for DST-FIST  
285 programme (SR/FST/College-2017/130 (c)). The project was supported by Researchers  
286 Supporting Project number (RSP-2021/231), King Saud University, Riyadh, Saudi Arabia.

287

288

289 **References**

- 290 [1] G.A.M. Amina, N.M. Spyrou; Study of gamma-radiation-induced optical effects in Ge–  
291 Se–Cd for possible industrial dosimetric applications. *Radiat. Phys. Chem.* 72 (2005)  
292 419–422
- 293 [2] L. Iannucci<sup>1</sup>, D. Pope; High velocity impact and armour design. *EXPRESS Polym. Lett.*  
294 5 (2011) 262–272
- 295 [3] L. S. Novikov, V. N. Mileev, E. N. Voronina, L. I. Galanina, A. A. Makletsov, and V. V.  
296 Sinolits; Radiation Effects on Spacecraft Materials. *J. Surf. Invest.: X-Ray . Synchrotron*  
297 *Neutron Tech.* 3 (2009) 199–214
- 298 [4] S.L Chinke, I.S Sandhu, T.M Bhawe, P.S Alegaonkar; Surface interactions of transonic  
299 shock waves with graphene-like nanoribbons, *Surfaces* 3 (2020) 505-515
- 300 [5] S. R. Alharbi, K.F.A. El-Rahman; Gamma Irradiation Effects On The Linear And  
301 Nonlinear Optical Properties Of Noncrystalline  $Sb_2S_3$  Films. *Chalcogenide Lett.* 14 (2017)  
302 529 – 537
- 303 [6] Gilles Buchs, Stefan Kundermann, Erwin Portuondo-Campa and Steve Lecomte;  
304 Radiation hard mode-locked laser suitable as a spaceborne frequency comb; *Opti.Exp.*  
305 23 (2015) 9890-9900
- 306 [7] M.A. Ahlam, M.N. Ravishankar, N. Vijayan, G. Govindaraj, Siddaramaiah, A.P. Gnana  
307 Prakash; Investigation of gamma radiation effect on chemical properties and surface  
308 morphology of some nonlinear optical (NLO) single crystals. *Nucl. Instrum. Methods*  
309 *Phys. Res. B* 278 (2012) 26–33

- 310 [8] Yongjun Dong, Jun Xu, Guoqing Zhou, Guangjun Zhao, Liangbi Su, Xiaodong Xu,  
311 Hongjun Li, JiLiang Si; Gamma-ray induced color centers in Yb:YAG crystals grown by  
312 Czochralski method. *Solid. State. Commun.* 141 (2007) 105–108
- 313 [9] Shamal L.Chinke, Inperpal S.Sandhu, Tejashree M.Bhave, Prashant S.Alegaonkar; Shock  
314 wave hydrodynamics of nano-carbons; *Mater. Chem.Phys* 263 (2020) 124337
- 315 [10] S.L.Chinke, I.S. Sandhu, D.R.Saroha, P.S Alegaonkar ; Graphene-like nanoflakes for  
316 shock absorption applications, *ACS Appl.Nano.Mater* 1 (2018) 6027-6037
- 317 [11] A. Rita, A. Sivakumar, S. Sahaya Jude Dhas, S. A. Martin Britto Dhas; Structural, optical  
318 and magnetic properties of silver oxide (AgO) nanoparticles at shocked conditions. *J.*  
319 *Nanostruc.Chem.* 10 (2020) 309–316.
- 320 [12] A. Sivakumar, S. Sahaya Jude Dhas, S.A. Martin Britto Dhas; Impact of shock waves on  
321 vibrational and structural properties of glycine phosphite. *Solid State Sci.*110 (2020)  
322 106452.
- 323 [13] V. Jayaram, K. P. J. Reddy; Catalytic Effect of CeO<sub>2</sub>-Stabilized ZrO<sub>2</sub> Ceramics with  
324 Strong Shock-Heated Mono- and Di-Atomic Gases. *J. Am. Ceram. Soc.* 99 (2016) 4128–  
325 4136.
- 326 [14] A. Sivakumar, S. Soundarya, S. Sahaya Jude Dhas, K. Kamala Bharathi, and S. A. Martin  
327 Britto Dhas; Shock Wave Driven Solid State Phase Transformation of Co<sub>3</sub>O<sub>4</sub> to CoO  
328 Nanoparticles. *J.Phys.Chem.C.* 124 (2020) 10755–10763.
- 329 [15] A. Sivakumar, S. Sahaya Jude Dhas, T. Pazhanivel, Abdulrahman I. Almansour, Raju  
330 Suresh Kumar, Natarajan Arumugam, C. Justin Raj, and S. A. Martin Britto Dhas; Phase  
331 Transformation of Amorphous to Crystalline of Multiwall Carbon Nanotubes by Shock  
332 Waves. *Cryst. Growth Des.* 21 (2021) 1617–1624.

- 333 [16] Zhen Chen, Shan Jiang, Thomas D. Sewell, Yong Gan, Suleiman Y. Oloriegbe, and  
334 Donald L. Thompson; Effects of copper nanoparticle inclusions on pressure-induced  
335 fluid-polynanocrystalline structural transitions in krypton. *J.Appl.Phys.*116 (2014)  
336 233506.
- 337 [17] J. Bystrzycki; Static recrystallization of shock-wave (explosively) deformed Fe-40 at%  
338 Al-Zr-B intermetallic. *Intermetallics* 8 (2000) 89-98.
- 339 [18] G. Bhagavannarayana, S. Parthiban, and Subbiah Meenakshisundaram; An Interesting  
340 Correlation between Crystalline Perfection and Second Harmonic Generation Efficiency  
341 on KCl- and Oxalic Acid-Doped ADP Crystals. *Cryst.Growth. Des* 8 (2008) 446–451.
- 342 [19] Yusuke Asakuma, Qin Li, H. Ming Ang, Moses Tade, Kouji Maeda, Keisuke Fukui; A  
343 study of growth mechanism of KDP and ADP crystals by means of quantum chemistry.  
344 *Appl.Sur.Sci.* 254 (2008) 4524–4530.
- 345 [20] S. Balamurugan, P. Ramasamy; Growth and characterization of unidirectional (100) KDP  
346 single crystal by Sankaranarayanan–Ramasamy (SR) method. *Spectrochimica Acta Part*  
347 *A.* 71 (2009) 1979–1983.
- 348 [21] A.Sivakumar, P.Eniya, S.Sahaya Jude Dhas,J. Kalyanasundar, P.Sivaprakash,  
349 S.Arumugam and S.A.Martin Britto Dhas; Shock Wave Induced Defect Engineering on  
350 Structural and Optical Properties of Pure and dye doped Potassium Dihydrogen  
351 Phosphate Crystals. *Z. Kristallogr.* 235 (2020) 193–202.
- 352 [22] A. Sivakumar, M .Manivannan, S. Sahaya Jude Dhas, J. Kalyana Sundar , M. Jose and  
353 S.A. Martin Britto Dhas; Tailoring the dielectric properties of KDP crystals by shock  
354 waves for microelectronic and optoelectronic applications. *Mater. Res. Express.* 6, (2019)  
355 086303.

- 356 [23] A.Sivakumar, S.Suresh, S.Balachandar, J.Thirupathy, J.Kalayana Sundar, S.A.Martin  
357 Britto Dhas; Effect of Shock Waves on Thermophysical properties of ADP and KDP  
358 crystals Optic.Laser.Tech. 111(2018) 284-289.
- 359 [24] A. Sivakumar, S. Sahaya Jude Dhas, S. A. Martin Britto Dhas; Shock wave-induced  
360 optical band gap engineering on pure and dye-doped potassium dihydrogen phosphate  
361 crystals. J.Mater.Sci: Mater.Electron. 31 (2020) 13704–13713.
- 362 [25] A.Sivakumar, S.Sahaya Jude Dhas, S.Balachandar and S.A.Martin Britto Dhas; Effect of  
363 shock waves on structural and dielectric properties of ammonium dihydrogen phosphate  
364 crystal. Z. Kristallogr. 234 (2019) 557–567.
- 365 [26] A.Sivakumar, A.Saranraj, S.Sahaya Jude Dhas, M.Jose, K.Kamala Bharathi, and S.A.  
366 Martin Britto Dhas; Modification of optical properties of ammonium dihydrogen  
367 phosphate crystal by employing shock waves. Opt.Eng. 58 (2019) 107101.
- 368 [27] J. H. Joshi, S.A.Martin Britto Dhas, D. K. Kanchan, M.J.Joshi, K.D.Parikh; Tailoring the  
369 low dielectric constant in glutamic acid doped ammonium dihydrogen phosphate single  
370 crystal by virtue of MPa shock waves for microelectronic applications: the complex  
371 impedance and modulus formulation studies. J.Mater.Sci.: Mater. Electron. 31 (2020)  
372 14859–14878.
- 373 [28] A.Sivakumar, A.Saranraj, S.Sahaya Jude Dhas and S.A.Martin Britto Dhas; Shock wave  
374 induced enhancement of optical properties of benzyl crystal. Mater. Res. Express. 6,  
375 (2019) 046205.
- 376 [29] A.Sivakumar, A. Saranraj S Sahaya Jude Dhas, M.Jose and S A. Martin Britto Dhas;  
377 Shock wave-induced defect engineering for investigation on optical properties of  
378 triglycine sulfate crystal. Opt.Eng. 58, (2019) 077104.



- 379 [30] A. Sivakumar, S.Reena Devi, S. Sahaya Jude Dhas, R. Mohan Kumar, K.Kamala  
380 Bharathi, and S. A. Martin Britto Dhas; Switchable Phase Transformation (Orthorhombic  
381 - Hexagonal) of Potassium Sulfate Single Crystal at Ambient Temperature by Shock  
382 Waves. *Cryst. Growth Des.* 20, (2020) 7111–7119.
- 383 [31] A.Sivakumar, M.Sarumathi, S.Sahaya Jude Dhas, S.A. Martin Britto Dhas; Enhancement  
384 of the optical properties of copper sulphate crystal by the influence of shock waves.  
385 *J.Mater.Res.* 428 (2020) 391-400.
- 386 [32] K. Showrilu, Ch. Jyothirmai, A.R.N.L.Sirisha, A. Sivakumar, S. Sahaya Jude Dhas, and  
387 S.A.Martin Britto Dhas; Shock wave-induced defect engineering on structural and optical  
388 properties of crown ether magnesium chloride potassium thiocyanate single crystal.  
389 *J. Mater. Sci.: Mater. Electron.* 32 (2021) 3903–3911.
- 390 [33] A. Sivakumar, S.Balachandar, S. A. Martin Britto Dhas; Measurement of “Shock Wave  
391 Parameters” in a Novel Table-Top Shock Tube Using Microphones. *Hum. Fact. Mech.*  
392 *Eng. Defense. Safety.* 4, (2020) 3.
- 393 [34] Takanori Fukami and Ruey-Hong Chen; Crystal Structure and Transitions for Monoclinic  
394  $\text{KH}_2\text{PO}_4$  Crystal. *J. Phys.Soc.Japan.* 75 (2006) 074602.
- 395 [35] Yan Ren, Xian Zhao, Edward W. Hagley, Lu Deng; Ambient-condition growth of high-  
396 pressure phase centrosymmetric crystalline KDP microstructures for optical second  
397 harmonic generation. *Sci. Adv.* 2 (2016) 1600404.
- 398 [36] J. Anand Subramony, Brian J. Marquardt, John W. Macklin, and Bart Kahr; Reevaluation  
399 of Raman Spectra for  $\text{KH}_2\text{PO}_4$  High-Temperature Phases. *Chem. Mater.* 11 (1999) 1312-  
400 1316.
- 401 [37] Weizhao Cai and Andrzej Katrusiak; Structure of the high-pressure phase IV of  $\text{KH}_2\text{PO}_4$

- 402 (KDP). Dalton Trans. 42 (2013) 863-866.
- 403 [38] Dongli Xu, Dongfeng Xue, Henryk Ratajczak; Morphology and structure studies  
404 of KDP and ADP crystallites in the water and ethanol solutions. J.Mole.Struct 740  
405 (2005) 37–45.
- 406 [39] J.H.Joshi, G.M.Joshi, M. J.Joshi, H.O.Jethvaa and K.D.Parikh; Raman,  
407 photoluminescence, and a.c. electrical studies of pure and L-serine doped ammonium  
408 dihydrogen phosphate single crystals: an understanding of defect chemistry in hydrogen  
409 bonding. New J. Chem. 42 (2018) 17227-17249.
- 410 [40] Hailiang Zhou, Fang Wang, Mingxia Xu, Baoan Liu, Fafu Liu, Lisong Zhang, Xinguang  
411 Xu, Xun Sun, Zhengping Wang; Raman spectral characterization of  $\text{NH}_4\text{H}_2\text{PO}_4$  single  
412 crystals: Effect of pH on microstructure. J.Cryst.Growth. 450 (2016) 6–13.
- 413 [41] A.Sivakumar, A. Saranraj, S.Sahaya Jude Dhas, K. Showrilu and S.A. Martin Britto  
414 Dhas. Phase stability analysis of shocked ammonium dihydrogen phosphate by X-ray and  
415 Raman scattering studies. Z. Kristallogr. 236 (2021) 1–10.
- 416
- 417
- 418
- 419

**Compliance with ethical standards**

None

**Conflict of interest**

The authors declare that they have no conflict of interest.

Journal Pre-proof